

Robust Single Rotation Averaging

Seong Hun Lee Javier Civera*
 I3A, University of Zaragoza, Spain
 {seonghunlee, jcivera}@unizar.es

Abstract

We propose a novel method for single rotation averaging using the Weiszfeld algorithm. Our contribution is three-fold: First, we propose a robust initialization based on the elementwise median of the input rotation matrices. Our initial solution is more accurate and robust than the commonly used chordal L_2 -mean. Second, we propose an outlier rejection scheme that can be incorporated in the Weiszfeld algorithm to improve the robustness of L_1 rotation averaging. Third, we propose a method for approximating the chordal L_1 -mean using the Weiszfeld algorithm. An extensive evaluation shows that both our method and the state of the art perform equally well with the proposed outlier rejection scheme, but ours is 2 – 4 times faster.

1. Introduction

We consider the problem of single rotation averaging, i.e., averaging several estimates of a single rotation to obtain the best estimate. This problem is relevant in many applications such as structure from motion (SfM) [7, 13], camera rig calibration [3], motion capture [12], satellite/spacecraft attitude determination [9, 10] and crystallography [8, 11].

A standard approach for single rotation averaging is to find the rotation that minimizes a cost function based on the distance to the input rotations. We refer to [6] for an extensive study of various distance functions. The current state-of-the-art method is to minimize the sum of geodesic distances using the Weiszfeld algorithm on $SO(3)$ [7].

In this work, we propose a novel method, also based on the Weiszfeld algorithm [14, 15], that is faster and more robust than [7]. Our contributions are as follows:

1. A robust initialization from the elementwise median of the input rotation matrices (Section 3.1).
2. An implicit outlier rejection scheme performed at each iteration of the Weiszfeld algorithm (Section 3.2).
3. An approximation of the chordal median in $SO(3)$ using the Weiszfeld algorithm (Section 3.3).

*This work was partially supported by the Spanish government (project PGC2018-096367-B-I00) and the Aragón regional government (Grupo DGA-T45.17R/FSE).

We substantiate our claim through extensive evaluation on synthetic data (Section 4). To download our Matlab code, go to <http://seonghun-lee.github.io>.

2. Preliminaries

We denote the vectorization of an $n \times m$ matrix by $\text{vec}(\cdot)$ and its inverse by $\text{vec}_{n \times m}^{-1}(\cdot)$. For a 3D vector \mathbf{v} , we define \mathbf{v}^\wedge as the corresponding 3×3 skew-symmetric matrix, and denote the inverse operator by $(\cdot)^\vee$, i.e., $(\mathbf{v}^\wedge)^\vee = \mathbf{v}$. The Euclidean, the L_1 and the Frobenius norm are respectively denoted by $\|\cdot\|$, $\|\cdot\|_1$ and $\|\cdot\|_F$. A rotation can be represented by a rotation matrix $\mathbf{R} \in SO(3)$ or a rotation vector $\mathbf{v} = \theta \hat{\mathbf{v}}$ where θ and $\hat{\mathbf{v}}$ are the angle and the unit axis of the rotation, respectively. The two representations are related by Rodrigues formula, and we denote the corresponding mapping between them by $\text{Exp}(\cdot)$ and $\text{Log}(\cdot)$ [5]:

$$\mathbf{R} = \text{Exp}(\mathbf{v}) := \mathbf{I} + \frac{\sin(\|\mathbf{v}\|)}{\|\mathbf{v}\|} \mathbf{v}^\wedge + \frac{1 - \cos(\|\mathbf{v}\|)}{\|\mathbf{v}\|^2} (\mathbf{v}^\wedge)^2, \quad (1)$$

$$\mathbf{v} = \text{Log}(\mathbf{R}) := \frac{\theta}{2 \sin(\theta)} (\mathbf{R} - \mathbf{R}^\top)^\vee \quad (2)$$

$$\text{with } \theta = \cos^{-1} \left(\frac{\text{tr}(\mathbf{R}) - 1}{2} \right). \quad (3)$$

The geodesic distance between two rotations $d_\angle(\mathbf{R}_1, \mathbf{R}_2)$ is obtained by substituting $\mathbf{R}_1 \mathbf{R}_2^\top$ into \mathbf{R} in (3). In [6], it was shown that the chordal distance is related to the geodesic distance by the following equation:

$$d_{\text{chord}}(\mathbf{R}_1, \mathbf{R}_2) := \|\mathbf{R}_1 - \mathbf{R}_2\|_F \quad (4)$$

$$= 2\sqrt{2} \sin(d_\angle(\mathbf{R}_1, \mathbf{R}_2)/2). \quad (5)$$

We define $\text{proj}_{SO(3)}(\cdot)$ as the projection of the 3×3 matrix onto the special orthogonal group $SO(3)$, which gives the closest rotation in the Frobenius norm [2]: For $\mathbf{M} \in \mathbb{R}^{3 \times 3}$,

$$\text{proj}_{SO(3)}(\mathbf{M}) := \mathbf{U} \mathbf{W} \mathbf{V}^\top, \quad (6)$$

where

$$\mathbf{U} \mathbf{\Sigma} \mathbf{V}^\top = \text{SVD}(\mathbf{M}), \quad (7)$$

$$\mathbf{W} = \begin{cases} \text{diag}(1, 1, -1) & \text{if } \det(\mathbf{U} \mathbf{V}^\top) < 0 \\ \mathbf{I}_{3 \times 3} & \text{otherwise} \end{cases}. \quad (8)$$

3. Method

3.1. Robust Initialization

In [7], the chordal L_2 mean of the rotations is taken as the starting point of the Weiszfeld algorithm. For input rotations $\{\mathbf{R}_i\}_{i=1}^N$, it is given by $\text{proj}_{SO(3)}\left(\sum_{i=1}^N \mathbf{R}_i\right)$ [6]. Although this initial solution can be obtained very fast, it is often inaccurate and sensitive to outliers. To overcome this weakness, we propose to initialize using the following matrix:

$$\mathbf{S}_0 = \underset{\mathbf{S} \in \mathbb{R}^{3 \times 3}}{\text{argmin}} \sum_{i=1}^N \sum_{j=1}^3 \sum_{k=1}^3 |(\mathbf{R}_i - \mathbf{S})_{jk}|, \quad (9)$$

where the subscript jk denote the element at the j -th row and the k -th column of the matrix. Note that $\sum_{j,k} |M_{jk}|$ is called the elementwise L_1 norm of the matrix \mathbf{M} . See Fig. 1 for the geometric interpretation of this distance metric. Since the nine entries of \mathbf{S} are independent, we can consider them separately in 1D space. Then, the entry of \mathbf{S}_0 at location (j, k) minimizes the sum of absolute deviations from the entries of \mathbf{R}_i 's at (j, k) , meaning that it is simply their median:

$$(\mathbf{S}_0)_{jk} = \text{median}\left(\{(\mathbf{R}_i)_{jk}\}_{i=1}^N\right) \text{ for all } j, k \in \{1, 2, 3\}. \quad (10)$$

The initial rotation matrix is then be obtained by projecting \mathbf{S}_0 onto $SO(3)$:

$$\mathbf{R}_0 = \text{proj}_{SO(3)}(\mathbf{S}_0). \quad (11)$$

3.2. Outlier Rejection in the Weiszfeld Algorithm

The geodesic L_1 -mean (i.e., median) of the rotations is defined as

$$\mathbf{R}_{\text{gm}} = \underset{\mathbf{R} \in SO(3)}{\text{argmin}} \sum_{i=1}^N d_{\angle}(\mathbf{R}_i, \mathbf{R}). \quad (12)$$

In [7], it was shown that this can be computed using the Weiszfeld algorithm on $SO(3)$ and that it is more robust to outliers than the L_2 -mean. However, a large number of outliers is still critical to the accuracy. To further mitigate the influence of the outliers, we modify the Weiszfeld algorithm of [7] such that the large residuals are given zero weight at each iteration. Specifically, we disregard all the residuals larger than $\max(d_{Q1}, d_{\max})$ where d_{Q1} is the first quartile of the residuals at each iteration and d_{\max} is some threshold we set in order to avoid discarding inliers. The details are given in Algorithm 1. A similar approach of disregarding large residuals was used in [4] for robust Perspective- n -Point (PnP) problem. Note that our approach contrasts [1] where a smooth robust cost function is favored for theoretically guaranteed convergence. In practice, our method is more robust to outliers (see Section 4.2).

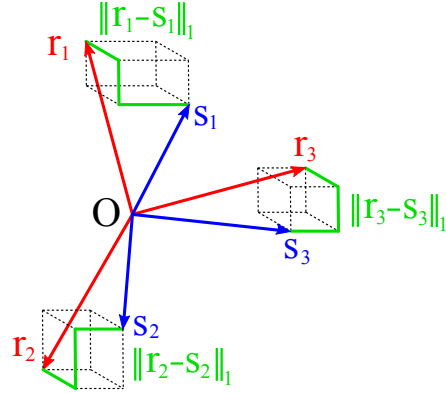


Figure 1. The elementwise L_1 norm of $(\mathbf{R} - \mathbf{S})$ is equal to $\sum_{i=1}^3 \|\mathbf{r}_i - \mathbf{s}_i\|_1$ where $\mathbf{R} = [\mathbf{r}_1, \mathbf{r}_2, \mathbf{r}_3]$ and $\mathbf{S} = [\mathbf{s}_1, \mathbf{s}_2, \mathbf{s}_3]$. This can be thought as the total length of the green lines.

3.3. Approximate Chordal L_1 -Mean

The chordal L_1 -mean of the rotations is defined as

$$\mathbf{R}_{\text{cm}} = \underset{\mathbf{R} \in SO(3)}{\text{argmin}} \sum_{i=1}^N d_{\text{chord}}(\mathbf{R}_i, \mathbf{R}). \quad (13)$$

In [6], a locally convergent algorithm on $SO(3)$ is proposed for this problem. In this work, we propose a different approach: Instead of iteratively updating the estimate on $SO(3)$, we first embed the rotations in a Euclidean space \mathbb{R}^9 , find their geometric median in \mathbb{R}^9 using the standard Weiszfeld algorithm [14, 15] (which is globally convergent), and then project this median onto $SO(3)$. In other words, we approximate \mathbf{R}_{cm} as

$$\mathbf{R}_{\text{cm}} \approx \text{proj}_{SO(3)}(\mathbf{S}_{\text{cm}}) \quad (14)$$

$$\text{with } \mathbf{S}_{\text{cm}} = \underset{\mathbf{S} \in \mathbb{R}^{3 \times 3}}{\text{argmin}} \sum_{i=1}^N \|\mathbf{R}_i - \mathbf{S}\|_F \quad (15)$$

$$= \text{vec}_{3 \times 3}^{-1} \left(\underset{\mathbf{s} \in \mathbb{R}^9}{\text{argmin}} \sum_{i=1}^N \|\text{vec}(\mathbf{R}_i) - \mathbf{s}\| \right). \quad (16)$$

Since the optimization is performed using the Weiszfeld algorithm, we can also incorporate the initialization and outlier rejection scheme in the previous sections. Algorithm 2 summarizes our method.

We point out two things in the implementation: First, since we do not optimize on $SO(3)$, the initial estimate does not have to come from a rotation, and we omit (11). Second, the threshold d_{\max} must be scaled appropriately when comparing Algorithm 1 and 2. Assuming that $\mathbf{s} \in \mathbb{R}^9$ at each iteration does not vastly differ from an embedding of a rotation in \mathbb{R}^9 , we convert d_{\max} from geodesic to chordal using (5), and vice versa. This is done in line 10 of Algorithm 2.

Algorithm 1: Geodesic median in $SO(3)$ [7] with outlier rejection

Input: List of rotation matrices $\{\mathbf{R}_i\}_{i=1}^N$
Output: \mathbf{R}_{gm}

```

/* Initialize (Section 3.1). */
1  $\mathbf{S}_0 \leftarrow \mathbf{0}_{3 \times 3}$ ;
2  $(\mathbf{S}_0)_{jk} \leftarrow \text{median}(\{(\mathbf{R}_i)_{jk}\}_{i=1}^N) \quad \forall j, k = 1, 2, 3$ ;
3  $\mathbf{R}_0 \leftarrow \text{proj}_{SO(3)}(\mathbf{S}_0)$ ;
/* Run the Weiszfeld algorithm on  $SO(3)$  [7]
with outlier rejection (Section 3.2). */
4  $\mathbf{R}_{\text{gm}} \leftarrow \mathbf{R}_0$ ;
5 for  $it = 1, 2, \dots, 10$  do
6   while  $\mathbf{R}_{\text{gm}} \in \{\mathbf{R}_i\}_{i=1}^N$  do
7      $\mathbf{R}_{\text{gm}} \leftarrow \mathbf{R}_{\text{perturb}} \mathbf{R}_{\text{gm}}$ ; // Perturb slightly
8      $\mathbf{v}_i \leftarrow \text{Log}(\mathbf{R}_i \mathbf{R}_{\text{gm}}^\top) \quad \forall i = 1, \dots, N$ ;
9      $d_i \leftarrow \|\mathbf{v}_i\| \quad \forall i = 1, \dots, N$ ;
10     $d_{Q1} \leftarrow Q_1(\{d_1, \dots, d_N\})$ ; // First quartile
11     $d_{\text{max}} \leftarrow \begin{cases} 1 & \text{if } N \leq 50 \\ 0.5 & \text{otherwise} \end{cases}$ 
12     $d_{\text{thr}} \leftarrow \max(d_{Q1}, d_{\text{max}})$ ;
13     $w_i \leftarrow \begin{cases} 1 & \text{if } d_i \leq d_{\text{thr}} \\ 0 & \text{otherwise} \end{cases} \quad \forall i = 1, \dots, N$ ;
14     $\Delta \mathbf{v} \leftarrow \frac{\sum_{i=1}^N w_i \mathbf{v}_i / d_i}{\sum_{i=1}^N w_i / d_i}$ ;
15     $\mathbf{R}_{\text{gm}} \leftarrow \text{Exp}(\Delta \mathbf{v}) \mathbf{R}_{\text{gm}}$ ;
16    if  $\|\Delta \mathbf{v}\| < 0.001$  then
17      break;
18 return  $\mathbf{R}_{\text{gm}}$ 

```

4. Results

4.1. Initialization

For evaluation, we generated a synthetic dataset where the inlier rotations follow a Gaussian distribution with $\sigma = 5^\circ$, and the outliers have uniformly distributed angles $\in [0, \pi]$ at random directions. Fig. 2 compares the average accuracy of the proposed initial solution (Section 3.1) and the chordal L_2 -mean [6] over 1000 runs. It can be seen that our solution is significantly better than the chordal L_2 mean unless the outlier ratio is extremely high (i.e., above 90%). On average, the L_2 chordal method takes $0.37 \mu\text{s}$ and ours $0.83 \mu\text{s}$ per rotation. This time difference is insignificant compared to the optimization that follows (see Tab. 1).

4.2. Comparison against [7]

Using the same setup as in previous section, we compare Algorithm 1 and 2, with and without the proposed outlier rejection scheme (Section 3.2). This time, we consider two

Algorithm 2: Approximate chordal median in $SO(3)$ with outlier rejection

Input: List of rotation matrices $\{\mathbf{R}_i\}_{i=1}^N$
Output: \mathbf{R}_{cm}

```

/* Initialize (Section 3.1). */
1  $\mathbf{S}_0 \leftarrow \mathbf{0}_{3 \times 3}$ ;
2  $(\mathbf{S}_0)_{jk} \leftarrow \text{median}(\{(\mathbf{R}_i)_{jk}\}_{i=1}^N) \quad \forall j, k = 1, 2, 3$ ;
/* Run the Weiszfeld algorithm in 9D space
with outlier rejection (Section 3.2). */
3  $\mathbf{s}_{\text{cm}} \leftarrow \text{vec}(\mathbf{S}_0)$ ;
4 for  $it = 1, 2, \dots, 10$  do
5   while  $\mathbf{s}_{\text{cm}} \in \{\text{vec}(\mathbf{R}_i)\}_{i=1}^N$  do
6      $\mathbf{s}_{\text{cm}} \leftarrow \mathbf{s}_{\text{cm}} + \mathcal{U}(0, 0.001)$ ; // Perturb
7      $\mathbf{v}_i \leftarrow \text{vec}(\mathbf{R}_i) - \mathbf{s}_{\text{cm}} \quad \forall i = 1, \dots, N$ ;
8      $d_i \leftarrow \|\mathbf{v}_i\| \quad \forall i = 1, \dots, N$ ;
9      $d_{Q1} \leftarrow Q_1(\{d_1, \dots, d_N\})$ ; // First quartile
10     $d_{\text{max}} \leftarrow \begin{cases} 2\sqrt{2} \sin(1/2) \approx 1.356 & \text{if } N \leq 50 \\ 2\sqrt{2} \sin(0.5/2) \approx 0.700 & \text{otherwise} \end{cases}$ 
11     $d_{\text{thr}} \leftarrow \max(d_{Q1}, d_{\text{max}})$ ;
12     $w_i \leftarrow \begin{cases} 1 & \text{if } d_i \leq d_{\text{thr}} \\ 0 & \text{otherwise} \end{cases} \quad \forall i = 1, \dots, N$ ;
13     $\mathbf{s}_{\text{cm,prev}} \leftarrow \mathbf{s}_{\text{cm}}$ ;
14     $\mathbf{s}_{\text{cm}} \leftarrow \frac{\sum_{i=1}^N w_i \mathbf{v}_i / d_i}{\sum_{i=1}^N w_i / d_i}$ ;
15    if  $\|\mathbf{s}_{\text{cm}} - \mathbf{s}_{\text{cm,prev}}\| < 0.001$  then
16      break;
17  $\mathbf{R}_{\text{cm}} = \text{proj}_{SO(3)}(\text{vec}_{3 \times 3}^{-1}(\mathbf{s}_{\text{cm}}))$ ;
18 return  $\mathbf{R}_{\text{cm}}$ 

```

different inlier noise levels, $\sigma = 5^\circ$ and 15° . The average accuracy of the evaluated methods¹ is compared in Fig. 3. With the outlier rejection, the geodesic L_1 -mean and our approximate chordal L_1 -mean are almost equally accurate. Without the outlier rejection, the geodesic L_1 -mean is more accurate than our approximate chordal L_1 -mean, but only for very high outlier ratios (i.e., $> 50\%$). Otherwise, there is no significant difference between the two.

The computation times are reported in Tab. 1. Our method is always faster than [7], and is 2–4 times faster with the outlier rejection. That said, the speed is not a major advantage, since all methods can process several hundreds of rotations in less than a millisecond. In most cases, averaging rotations will take much less time than other operations, such as the computation of input rotations.

¹We did not include the chordal L_2 -mean here, since it produced much larger errors than the rest and was already reported in Fig. 2.

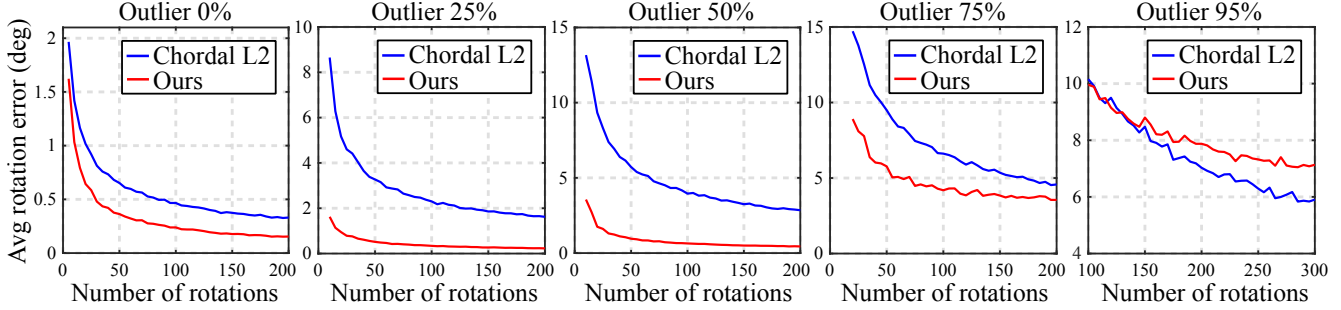


Figure 2. Average rotation errors of different initialization methods: Chordal L_2 -mean [7] versus ours (Section 3.1).

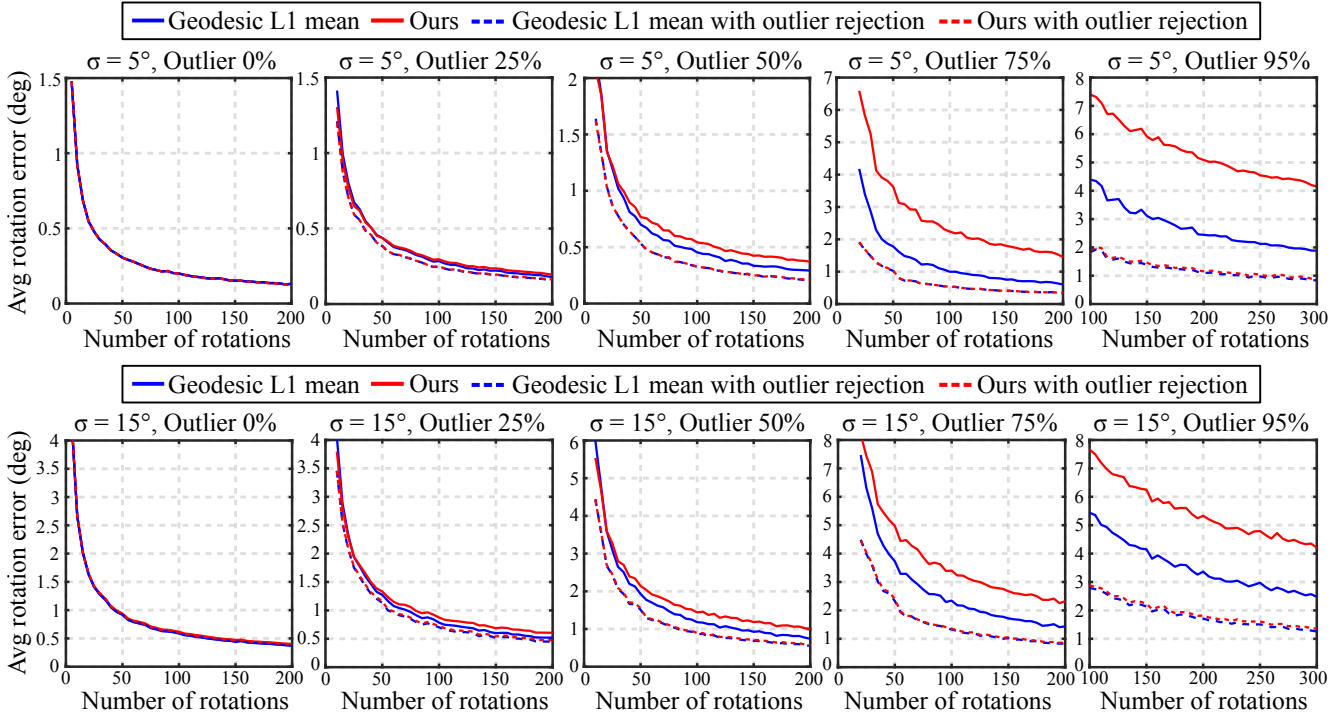


Figure 3. Average rotation errors of geodesic L_1 -mean [7] versus ours (Section 3.3), with and without the outlier rejection (Section 3.2).

5. Conclusions

In this work, we proposed a novel alternative to the work of Hartley et al. [7] for robust single rotation averaging. While both our method and [7] use the Weiszfeld algorithm, there are three key differences:

1. We initialize the Weiszfeld algorithm using the elementwise median of the input rotation matrices.
2. We implicitly disregard the outliers at each iteration of the Weiszfeld algorithm.
3. We approximate the chordal median on $SO(3)$ instead of the geodesic median as in [7].

As a result, our method achieves better performance in terms of speed and robustness to outliers. We also found that incorporating the proposed outlier rejection in the original implementation of [7] leads to similar performance, but at 2–4 times slower than ours.

	w/o outlier rejection		w/ outlier rejection	
	[7]	Ours	[7]	Ours
(5°, 0%)	8.69	4.38 (2.0×)	9.37	4.43 (2.1×)
(5°, 25%)	10.5	4.47 (2.3×)	11.7	5.68 (2.1×)
(5°, 50%)	15.2	6.21 (2.4×)	17.2	6.78 (2.5×)
(5°, 75%)	24.9	15.2 (1.6×)	27.2	7.71 (3.5×)
(5°, 95%)	32.1	10.3 (3.1×)	31.6	8.99 (3.5×)
(15°, 0%)	10.7	6.00 (1.8×)	17.0	6.02 (2.8×)
(15°, 25%)	15.0	5.98 (2.5×)	17.0	7.1 (2.4×)
(15°, 50%)	19.6	7.66 (2.6×)	22.3	8.06 (2.8×)
(15°, 75%)	24.9	11.1 (2.2×)	28.1	8.77 (3.2×)
(15°, 95%)	29.1	10.2 (2.9×)	31.7	8.50 (3.7×)

Table 1. Median computation time (μs /rotation) under different outlier noise levels and outlier ratios. The speedup compared to [7] is given in parentheses. All algorithms were implemented in MATLAB and run on a laptop CPU (Intel i7-4810MQ, 2.8 GHz).

References

- [1] K. Aftab and R. Hartley. Convergence of iteratively re-weighted least squares to robust m-estimators. In *IEEE Winter Conf. on Applications of Computer Vision*, pages 480–487, 2015. [2](#)
- [2] K. S. Arun, T. S. Huang, and S. D. Blostein. Least-squares fitting of two 3-D point sets. *IEEE Trans. Pattern Anal. Mach. Intell.*, 9(5):698–700, 1987. [1](#)
- [3] Yuchao Dai, Jochen Trumpf, Hongdong Li, Nick Barnes, and Richard Hartley. Rotation averaging with application to camera-rig calibration. In *Asian Conf. on Computer Vision*, pages 335–346, 2009. [1](#)
- [4] Luis Ferraz, Xavier Binefa, and Francesc Moreno-Noguer. Very fast solution to the pnp problem with algebraic outlier rejection. In *Proc. IEEE Computer Society Conf. on Computer Vision and Pattern Recognition (CVPR)*, pages 501–508, 2014. [2](#)
- [5] Christian Forster, Luca Carlone, Frank Dellaert, and Davide Scaramuzza. On-manifold preintegration for real-time visual-inertial odometry. *IEEE Trans. Robot.*, 33(1):1–21, 2017. [1](#)
- [6] Richard Hartley, Jochen Trumpf, Yuchao Dai, and Hongdong Li. Rotation averaging. *International Journal of Computer Vision*, 2013. [1](#), [2](#), [3](#)
- [7] Richard I. Hartley, Khurram Aftab, and Jochen Trumpf. L1 rotation averaging using the Weiszfeld algorithm. In *IEEE Conf. on Computer Vision and Pattern Recognition (CVPR)*, pages 3041–3048, 2011. [1](#), [2](#), [3](#), [4](#)
- [8] M. Humbert, N. Gey, J. Muller, and C. Esling. Determination of a Mean Orientation from a Cloud of Orientations. Application to Electron Back-Scattering Pattern Measurements. *Journal of Applied Crystallography*, 29(6):662–666, 1996. [1](#)
- [9] Q. M. Lam and J. L. Crassidis. Precision attitude determination using a multiple model adaptive estimation scheme. In *IEEE Aerospace Conference*, pages 1–20, 2007. [1](#)
- [10] Landis Markley, Yang Cheng, John Crassidis, and Yaakov Oshman. Averaging quaternions. *Journal of Guidance, Control, and Dynamics*, 30:1193–1196, 07 2007. [1](#)
- [11] A. Morawiec. A note on mean orientation. *Journal of Applied Crystallography*, 31(5):818–819, 1998. [1](#)
- [12] Inna Sharf, Alon Wolf, and M.B. Rubin. Arithmetic and geometric solutions for average rigid-body rotation. *Mechanism and Machine Theory*, 45(9):1239 – 1251, 2010. [1](#)
- [13] Roberto Tron, Xiaowei Zhou, and Kostas Daniilidis. A survey on rotation optimization in structure from motion. In *IEEE Conf. on Computer Vision and Pattern Recognition Workshops*, pages 1032–1040, 2016. [1](#)
- [14] Andre Weiszfeld. Sur le point pour lequel la somme des distances de n points donnés est minimum. *Tohoku Mathematical Journal*, 43:355–386, 1937. [1](#), [2](#)
- [15] Andre Weiszfeld and Frank Plastria. On the point for which the sum of the distances to n given points is minimum. *Annals of Operations Research*, 167(1):7–41, 2009. [1](#), [2](#)